SCIENTIFIC REPORTS

OPEN

SUBJECT AREAS:
DEVELOPMENT
CELLULAR NEUROSCIENCE
GENE EXPRESSION
MOLECULAR NEUROSCIENCE

Received
23 November 2011

Accepted
31 May 2012

Published
2 July 2012

Correspondence and requests for materials should be addressed to S.K. (kindler@uke.de)

* Current address: Department of Neurobiology, Max-Planck-Institute for Biophysical Chemistry, Am Faßberg 11, D-37077 Göttingen, Germany.

Synthesis of two SAPAP3 isoforms from a single mRNA is mediated via alternative translational initiation

John Jia En Chua[1]*, Claudia Schob[1], Monika Rehbein[1], Christos G. Gkogkas[3], Dietmar Richter[2] & Stefan Kindler[1]

[1]Institute for Human Genetics, [2]Center for Molecular Neurobiology, University Medical Center Hamburg-Eppendorf, Martinistr. 52, D-20246 Hamburg, Germany, [3]McGill Life Sciences Complex, Rosalind and Morris Goodman Cancer Centre, Montréal, H3A 1A3, Québec, Canada.

In mammalian neurons, targeting and translation of specific mRNAs in dendrites contribute to synaptic plasticity. After nuclear export, mRNAs designated for dendritic transport are generally assumed to be translationally dormant and activity of individual synapses may locally trigger their extrasomatic translation. We show that the long, GC-rich 5′-untranslated region of dendritic SAPAP3 mRNA restricts translation initiation via a mechanism that involves an upstream open reading frame (uORF). In addition, the uORF enables the use of an alternative translation start site, permitting synthesis of two SAPAP3 isoforms from a single mRNA. While both isoforms progressively accumulate at postsynaptic densities during early rat brain development, their levels relative to each other vary in different adult rat brain areas. Thus, alternative translation initiation events appear to regulate relative expression of distinct SAPAP3 isoforms in different brain regions, which may function to influence synaptic plasticity.

Translation initiation of most mRNAs involves the 7-methylguanosine cap (5′cap)-dependent recruitment of the 43 S complex that consists of the small ribosomal subunit, eukaryotic initiation factor (eIF) 3, eIF1/eIF1A and the eIF2–Met-tRNAi–GTP ternary complex[1,2]. The 43 S complex then scans the 5′-untranslated region (UTR). Upon recognition of an AUG initiation codon, GTP bound to the α subunit of eIF2 (eIF2α) is hydrolyzed. This allows the recruitment of the 60 S ribosomal subunit and the subsequent formation of the 80 S elongation-competent complex. AUG triplets presented in the context of a so-called Kozak sequence ((GCC)GCC$^{A}/_{G}$CCAUGG) are the most efficient sites for translation initiation[3,4]. At strong initiator sites, nucleotides at positions −3 and/or +4 (the A of the AUG codon is designated +1) match the Kozak sequence and enable most scanning 43 S complexes to initiate translation at this location. In contrast, 43 S complexes will more often skip AUG triplets presented in a less favorable context (leaky scanning), continue scanning and initiate translation at a downstream start codon[5,6].

Several intrinsic features of the 5′ UTR can influence the efficiency of translation initiation. Stable secondary structures within the 5′UTR often stall the linear movement of scanning 43 S complexes and inhibit translation initiation[7–9]. Similarly uORFs, short reading frames with start codons (uAUGs) residing in the 5′UTR, may decrease initiation efficiency at the authentic start codon (AUG^{+1}) of the main open reading frame (mORF)[7,10]. This is because ribosomes completing translation of a uORF may dissociate from the mRNA and the mORF located downstream will not be translated[11,12]. Alternatively, the post-termination 40 S subunit may remain attached to the mRNA after translating the uORF, resume scanning and reinitiate translation at a downstream start codon[13,14]. Reinitiation efficiency depends on several parameters such as the length of the uORF, the distance and sequence between the uAUG and the downstream initiation site and the physiological condition of the cell[13–18]. On the other hand, the 43 S complex may also skip the uAUG by leaky scanning and continue onwards to initiate translation at AUG^{+1} thereby enabling the synthesis of the full-length protein. However, if the uORF and the mORF overlap, ribosomes translating the former will bypass AUG^{+1} and will thus not be able to translate the complete mORF. In rare instances, alternative translation initiation (ATI) by reinitation at a downstream start codon in-frame with AUG^{+1} may yield an N-terminally shortened isoform. Such a uORF can enable the synthesis of several isoforms from a single mRNA[19,20].

Sustained translation initiation depends on the continued cycling of eIF2 between the GTP- and GDP-bound state[2]. Phosphorylation of eIF2α at Serine 51 prevents GDP/GTP exchange, reduces initiation events and consequently inhibits general translation. Paradoxically, increased phospho-eIF2α levels enhance the synthesis of proteins encoded by certain mRNAs that typically possess several uORFs[13,14,21]. After translating a uORF, a portion of the post-termination 40 S complexes can resume scanning, rebind the ternary complex and then reinitiate translation at a downstream uAUG. Successive reading of several uORFs strongly restricts the number of 43 S complexes reaching AUG^{+1} and therefore inhibits translation of the mORF. Phosphorylation of eIF2α lowers the levels of GTP-bound eIF2α. This increases the likelihood that post-termination 40 S subunits resuming scanning will bypass remaining uORFs and not re-acquire a ternary complex before reaching AUG^{+1}. Such a mechanism increases the probability that a reinitiating 43 S complex will translate the mORF and explains the unusual increase in the levels of proteins synthesized from these transcripts. Importantly, synaptic activity is known to control the levels of phospho-eIF2α in neurons[22,23] and the phosphorylation status of eIF2α bidirectionally modulates both synaptic plasticity and memory storage[24].

In mammalian neurons, a subset of mRNAs are specifically targeted to dendrites[25,26]. These mRNAs are believed to be kept in a translationally dormant state after exiting the nucleus until specific synaptic signals initiate local protein synthesis at synapses. The molecular details of this regulation are only partially understood[27–29]. For example, several dendritic transcripts initiate translation in a 5′cap-independent manner using so-called internal ribosome entry sites (IRESs)[30] that recruit ribosomes directly to a start codon without the assembly of initiation factors at the 5′-end of the mRNA[31,32]. Importantly, many dendritically localized mRNAs encode proteins that are highly concentrated at postsynaptic densities (PSDs), such as SAPAP3[33,34], different Shank/ProSAP family members (Shanks)[35] and PSD-95/SAP90[36,37]. PSDs are dense cytoplasmic protein signaling networks associated with the postsynaptic membrane of excitatory synapses[38–40]. SAPAP3, Shanks and PSD-95 are master scaffolding proteins of the PSD that cross-link neurotransmitter receptors, signaling molecules and cytoskeletal components[41–43]. While SAPAP3 mRNAs have not yet been shown to be specifically translated at synapses, an activity triggered local synthesis of PSD components at synapses is generally believed to induce a reorganization of the postsynaptic signal transduction machinery and thereby regulate synaptic plasticity[27]. Consistently, SAPAP3 knockout mice exhibit a behavior reminiscent of obsessive-compulsive disorder in humans suggesting that a tight control of SAPAP3 levels in mammalian brain neurons is essential to maintain normal synaptic physiology[44]. Here we show that the regulation of SAPAP3 levels is exerted at the level of translation. A particular uORF strongly down-regulates translation efficiency while also enabling the synthesis of two distinct SAPAP3 isoforms via alternative translation initiation.

Results

The 5′UTR of SAPAP3 mRNAs down-regulates translation. 5′UTRs are involved in regulating translation initiation, a major point of translation control. To investigate regulatory effects of the 5′UTR of rat SAPAP3 mRNAs (S3-5′UTR), we first determined its complete sequence. A 5′RACE product obtained from adult rat brain cDNA encodes a 295 nt GC-rich (72%) 5′UTR that is highly conserved in mouse, dog and human (Fig. 1A) and includes four uORFs and 104 nt of the previously reported rat SAPAP3 cDNA (NM_173138). To assess if the S3-5′UTR contains an IRES, bicistronic transcripts encoding separate *Photinus* (PhoLuc) and *Renilla* luciferase (RenLuc) ORFs connected via different intervening sequences were expressed in HEK293 cells and primary cortical neurons. IRES activity is defined as PhoLuc to RenLuc activity ratio (Pho:Ren ratio) with the quotient obtained with the basic mRNA containing a synthetic 29 nt intervening sequence set to 1. While known IRES elements from *Encephalomyocarditis* virus (EMCV) or Arc/arg3.1 mRNAs[30] produced Pho:Ren ratios of about 4 or higher, Pho:Ren ratios below 1 clearly showed that the S3-5′UTR exhibits no IRES activity in both cell systems (see Supplementary Fig. S1 online).

To further examine the translation regulatory potential of the S3-5′UTR, mammalian cells were transfected with various eukaryotic expression vectors. pEGFP-N3 encodes mRNAs consisting of a 92 nt synthetic 5′UTR, the enhanced green fluorescent protein (EGFP) ORF and a 192 nt 3′UTR partially derived from the SV40 early mRNA. The 5′UTR is short, contains no uORFs and enables efficient translation. p5′S3-EGFP transcripts are identical but additionally contain the S3-5′UTR plus the first eight codons of SAPAP3 mRNAs inserted upstream of and in-frame with the EGFP ORF. One day after transfection, pEGFP-N3 transfected HEK293 cells and neurons exhibited strong autofluorescence while only very little EGFP fluorescence was observed in p5′S3-EGFP transfected cells (Fig. 1B&C). Thus, in comparison to the synthetic 5′UTR, the S3-5′UTR appears to strongly reduce translation in neuronal and non-neuronal cells.

What mechanism underlies translational down-regulation? We tested transcripts derived from three different vectors all containing an ORF encoding FLAG-tagged SAPAP3 and the complete 644 nt SAPAP3 3′UTR (S3-3′UTR; GenBank accession number FJ705274). However, each vector possesses distinct 5′UTRs: i) a synthetic 28 nt element supporting efficient translation (pFS3), ii) the S3-5′UTR (pS3-FS3) and iii) the 5′UTR of rat SAPAP1 mRNAs (S1-5′UTR, pS1-FS3). While similar in length to the S3-5′UTR the 274 nt S1-5′UTR only has a 50% GC content. Northern blot analysis with RNA from transfected HEK293 cells revealed that all three recombinant mRNAs are present at comparable concentrations (Fig. 2A) indicating that the distinct 5′UTRs do not lead to different transcript levels. However, while pFS3 and pS1-FS3 transfected cells contained comparable FLAG-SAPAP3 levels as observed by Western blotting, the recombinant protein was barely detectable in extracts of cells synthesizing the S3-5′UTR containing mRNA (Fig. 2B). Thus, in contrast to the S1-5′UTR, the S3-5′UTR strongly down-regulates translation efficiency.

Translation control often involves interactions between 5′ and 3′UTRs[45–47]. To assess the regulatory effect of both S3-5′UTR and S3-3′UTR, HEK293 cells and cortical neurons were co-transfected with pLUC-based constructs and pREN encoding PhoLuc and RenLuc, respectively. Luciferase activities were then determined from cell extracts. The Pho:Ren ratio of pLUC transfected cells synthesizing mRNAs containing a 87 nt synthetic 5′UTR, the PhoLuc ORF and a 294 nt 3′UTR partially derived from the bovine growth hormone (BGH) mRNA was set to 100%. Pho:Ren ratios of cells transfected with other constructs were calculated as percentage of this value (nPho:Ren ratio). Replacing the BGH 3′UTR with the S3-3′UTR (pS33-LUC) did not alter the nPho:Ren ratio in neurons and led to only a slight reduction (28%) in HEK293 cells (Fig. 2C). In contrast, swapping the synthetic 5′UTR for the S3-5′UTR (pS35-LUC) drastically reduced the nPho:Ren ratio in both neurons (95%) and HEK293 cells (97%). In both cells systems, the additional exchange of the BGH 3′UTR for the S3-3′UTR (pS353-LUC) did not significantly alter the S3-5′UTR mediated reduction of the nPho:Ren ratio. Thus, the S3-5′UTR strongly reduces translation efficiency in neuronal and non-neuronal cells without significant contribution from the S3-3′UTR. These findings were supported by luciferase assays performed in reticulocyte lysates programmed with *in vitro* transcribed capped mRNAs. PhoLuc activity achieved with 25 ng and 1 μg pS35-LUC mRNA is only about 3% and 1%, respectively, of the PhoLuc activity obtained with the same amount of pLUC mRNA.

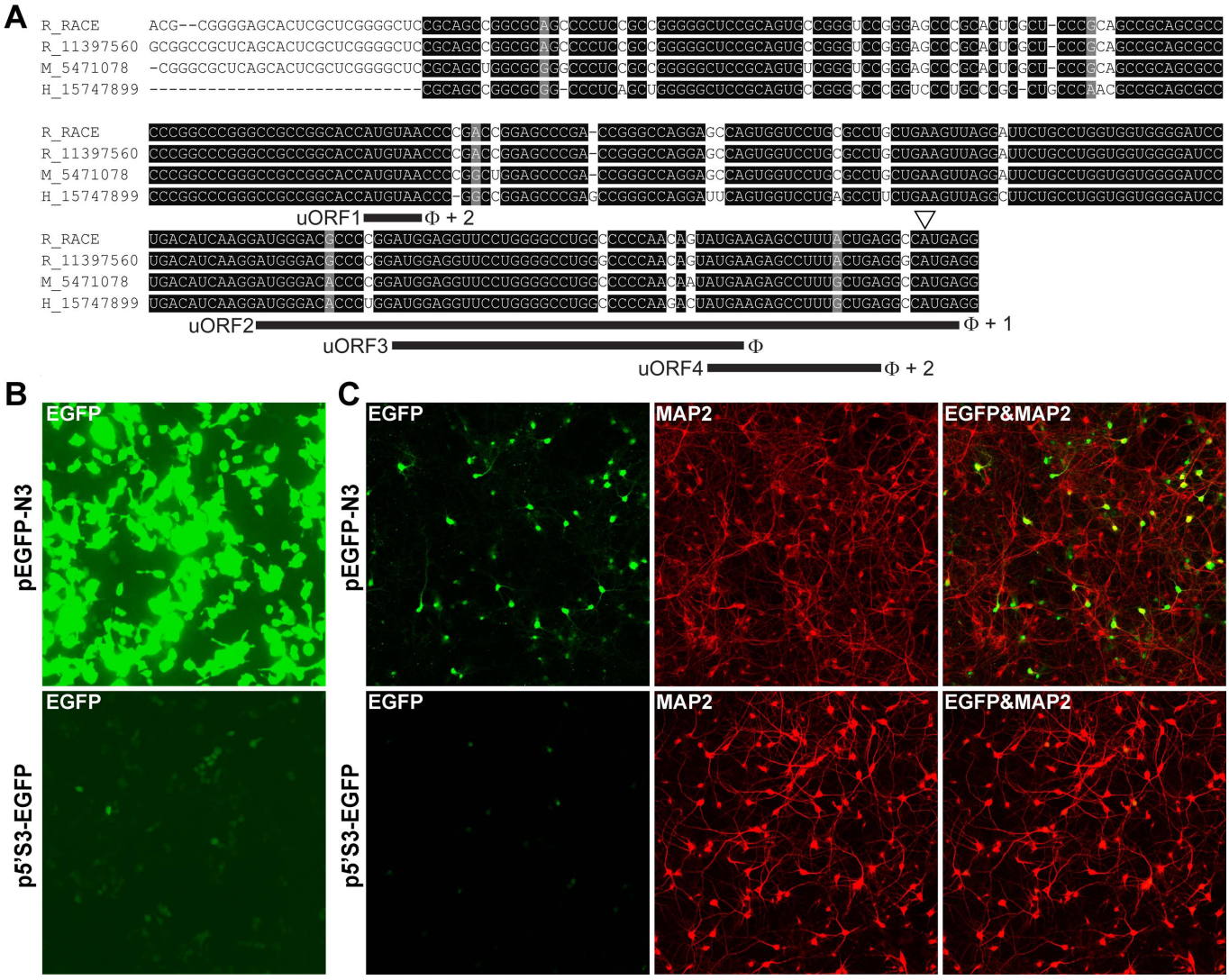

Figure 1 | Evolutionarily Conserved 5′UTR of SAPAP3 mRNAs Down-Regulates Translation. (A) Alignment of 5′UTR sequences from rat, mouse (GenBank accession number AI836865) and human (BI756308) SAPAP3 mRNAs indicating the AUG start codon of the SAPAP3 ORF (▽), conserved nucleotides (highlighted by a black background) and four conserved uORFs (underlined; uORF phases are indicated relative to the phase of the SAPAP3 ORF (Φ)). (B&C) HEK293 cells (B) and rat cortical neurons (C) transfected with pEGFP-N3 exhibit strong EGFP fluorescence (upper panels, green channel), whereas EGFP levels are drastically reduced in cells transfected with p5′S3-EGFP (lower panels, green channel). Identical exposure times were used to detect EGFP. In primary neurons somatodendritic microtubule-associated protein 2 (MAP2) is detected by immunocytochemistry (red channel). Two-channel overlay pictures (C, right panels) indicate that transfected neurons are normally differentiated.

uORF mediated translational down-regulation. Down-regulation of translation efficiency is often mediated via uORFs or stable secondary structures within 5′UTRs[7,10]. Stem-loop formations with ΔG values below −50 kcal/mol often inhibit translation by stalling 43 S pre-initiation complex scanning of the 5′UTR[9]. MFold predicts that the S3-5′UTR folds into a stable secondary structure with a ΔG of about −150 kcal/mol (see Supplementary Fig. S2 online). Does the predicted conformation contribute to translational down-regulation? Three pS3-FS3-based vectors encoding mRNAs harboring distinct deletions within the S3-5′UTR were constructed to address this question (Fig. 3A). Deleting nt 53–124 (pS3Δ53-124-FS3), 1–150 (pS3Δ150-FS3) and 1–203 (pS3Δ203-FS3) from the S3-5′UTR changes the ΔG values of the predicted secondary structures to about −100, −58 and −27 kcal/mol, respectively. Cell lysates of HEK293 cells co-transfected with pEGFP-N3 and one of the pS3-FS3-based vectors were analyzed by Western blotting with anti-EGFP and anti-FLAG antibodies (Fig. 3B). Comparable EGFP levels in all tested lysates indicate similar transfection efficiencies. However, FLAG-SAPAP3 was highly concentrated in pFS3 transfected cells but only weakly detected in cells expressing mRNAs containing either the complete S3-5′UTR or truncated versions thereof. Thus, the proximal 90 nt of the S3-5′UTR are sufficient for translational down-regulation. Since the ΔG value predicted for the secondary structure of this truncated 5′UTR is about −27 kcal/mol, the S3-5′UTR appears to down-regulate translation efficiency by a mechanism unrelated to stalling of 43 S complex scanning by strong secondary structures.

Are the four evolutionarily conserved uORFs of the S3-5′UTR involved in translational control? Whereas uORF1 consists of only a start and a stop codon uORF2, uORF3 and uORF4 encode peptides spanning 23, 11 and 5 amino acids, respectively. Of the four uORFs, only uORF3 is in-frame with the SAPAP3 ORF (S3-ORF) while only uORF2 overlaps with the S3-ORF (Fig. 3A). The first two nt of the uORF2 stop codon also represent the last two nt of the SAPAP3 start codon (AUGA, Fig. 1). NetStart (www.cbs.dtu.dk/services/NetStart/) predicts that uAUG2 and uAUG3 can indeed function as translation

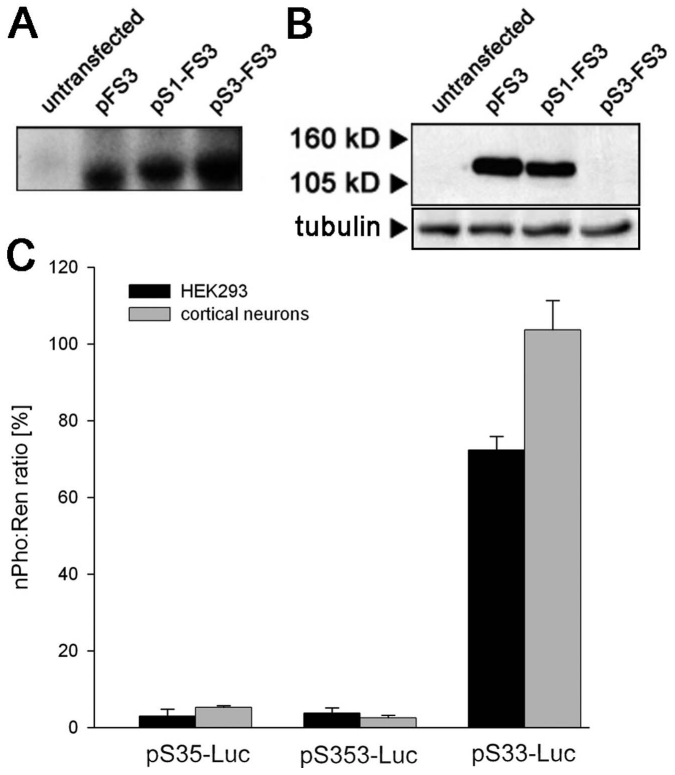

Figure 2 | The 5′UTR of Rat SAPAP3 mRNAs Down-Regulates Translation Efficiency. (A) The 5′UTRs of SAPAP1 and SAPAP3 transcripts do not alter mRNA levels. In 10 μg total RNA isolated from control or transfected HEK293 cells recombinant transcripts were detected via Northern blotting with a SAPAP3 cDNA probe. (B) The 5′UTR of SAPAP3 but not SAPAP1 mRNAs down-regulates translation. In protein extracts (10 μg) from untransfected and transfected cells FLAG-SAPAP3 was detected by Western blotting with an anti-FLAG tag antibody. Endogenous α-tubulin was detected as a loading control. (C) The 3′UTR of SAPAP3 mRNAs does not alter translation. Extracts from transfected HEK293 cells and cortical neurons were assayed for luciferase activities. Standard deviations were obtained from three independent experiments.

start sites (Table 1). To determine whether uORF2 and uORF3 interfere with translation initiation at AUG^{+1}, the translation efficiency of puORF2+3^{AAG}-Δ150-FS3 transcripts, in which uAUG2 and uAUG3 were converted into AAG triplets was examined in transfected HEK293 cells (Fig. 3B). In contrast to the weak FLAG-SAPAP3 synthesis from pS3Δ150-FS3 derived mRNAs, both puORF2+3^{AAG}-Δ150-FS3 and pFS3 transcripts lead to high FLAG-SAPAP3 levels. Disruption of only uORF2 in the context of the entire S3-5′UTR (puORF2^{AAG}-S3-FS3; Fig. 3C) completely abolished the down-regulation of FLAG-SAPAP3 synthesis while disruption of only uORF3 (puORF3^{AAG}-S3-FS3) had no effect. Note that the point mutation in puORF2^{AAG}-S3-FS3 transcripts does not change the predicted ΔG value of the S3-5′UTR. Thus, S3-5′UTR-mediated down-regulation of FLAG-SAPAP3 synthesis results from the translation of uORF2. Since uORF2 overlaps with the S3-ORF, ribosomes translating uORF2 bypass AUG^{+1} and are thus unable to synthesize full-length SAPAP3.

uORF2 mediates synthesis of two distinct SAPAP3 isoforms from a single mRNA. Transcripts of pFS3-based vectors contain regions that are not present in SAPAP3 mRNAs, such as the FLAG-ORF. To eliminate all effects possibly mediated by these sequences, we performed experiments with constructs derived from pS3-S3, a vector encoding the full-length authentic SAPAP3 mRNA. Lysates from transfected HEK293 cells were analyzed by Western blotting utilizing a SAPAP3 antiserum (Fig. 3D). SAPAP3 was very efficiently synthesized from pS3 transcripts, in which the S3-5′UTR was replaced by a short synthetic 5′UTR. In comparison, authentic SAPAP3 mRNAs (pS3-S3) or identical transcripts missing nt 1–150 (pS3Δ150-S3) and 1–203 (pS3Δ203-S3) yielded strongly diminished SAPAP3 levels (Fig. 3D, ~130 kDa band designated "SAPAP3α"). However, disruption of both uORF2 and uORF3 in pS3Δ203-S3 transcripts (puORF2+3^{AAG}-Δ203-S3) restored the SAPAP3α concentration to levels observed in pS3-transfected cells. Interestingly, cells expressing mRNAs containing the complete (pS3-S3) or a truncated S3-5′UTR (pS3Δ150-S3 and pS3Δ203-S3) produce a second SAPAP3 isoform with an apparent molecular weight of ~110 kDa ("SAPAP3β"). Yet, SAPAP3β is neither synthesized from an mRNA in which both uORF2 and uORF3 are disrupted (puORF2+3^{AAG}-Δ203-S3) nor from transcripts totally lacking S3-5′UTR sequences (pS3). Thus, uORF2 and/or uORF3 are required for SAPAP3β synthesis while partially suppressing SAPAP3α synthesis. Mutation of only uAUG3 in full-length SAPAP3 mRNAs (puORF3^{AAG}-S3) did not alter the SAPAP-3α:SAPAP3β level ratio (α:β ratio) as compared to authentic SAPAP3 mRNAs, while the single disruption of uORF2 (puORF2^{AAG}-S3) shifted the ratio in favor of SAPAP3α. Co-migration of SAPAP3α and FLAG-SAPAP3 suggests that translation of the full-length S3-ORF leads to SAPAP3α. Remarkably, rat PSD preparations contain two SAPAP3 isoforms co-migrating with SAPAP3α and SAPAP3β synthesized in transfected cells (Fig. 3E). Taken together, these data suggest that two distinct SAPAP3 isoforms are synthesized from a single mRNA, in which uORF2 down-regulates SAPAP3α synthesis in favor of SAPAP3β synthesis.

Alternative start codons mediate synthesis of two SAPAP3 isoforms. The synthesis of two SAPAP3 isoforms may result from ATI involving two parallel scenarios: i) ribosomes scanning the S3-5′UTR skip uAUG2 (leaky scanning) and initiate SAPAP3α synthesis at AUG^{+1}; ii) ribosomes translating uORF2 bypass AUG^{+1}, reinitiate translation at a downstream AUG and thus synthesize SAPAP3β. NetStart predicts that the in-frame triplets AUG^{+67} and AUG^{+277} are suitable for translation initiation (Table 1). To determine if one of these AUGs directs SAPAP3β synthesis, two pS3-derived vectors containing deletions of coding sequence nucleotides 1–66 (pΔAUG^{+1}-S3) and 1–276 (pΔAUG^{+67}-S3) of the S3-ORF (Fig. 4A), respectively, were transfected into HEK293 cells. Western blot analysis revealed that mRNAs in which either AUG^{+1} alone or AUG^{+1} and AUG^{+67} together are deleted lead to the synthesis of a protein co-migrating with SAPAP3β translated from pS3Δ150-S3 transcripts (Fig. 4B). In addition, when AUG^{+277} was mutated to an AAC triplet in pS3-S3, the resulting vector pS3-S3$^{+277AAC}$ still led to the synthesis of SAPAP3α but not SAPAP3β (Fig. 4C). Thus, SAPAP3β synthesis appears to start at AUG^{+277}. Interestingly, an additional protein intermediate in size between SAPAP3α and SAPAP3β is synthesized in minute amounts from pΔAUG^{+1}-S3 transcripts but not pΔAUG^{+67}-S3 mRNAs and is likely to result from rare translation initiation at AUG^{+67}. Taken together, different mechanisms appear to contribute to the synthesis of two SAPAP3 isoforms from a mutual mRNA. Leaky scanning of 43 S complexes past all four uAUGs and subsequent translation initiation at AUG^{+1} mediates SAPAP3α synthesis. In contrast, ribosomes translating uORF2 bypass AUG^{+1}, stop translation shortly thereafter and may subsequently reinitiate translation at AUG^{+277} leading to SAPAP3β synthesis. Noteworthy, the first 300 nt of the SAPAP3 mORF are highly conserved in various vertebrate species (see Supplementary Fig. S3 online).

SAPAP3 isoform concentrations differ in distinct rodent brain regions. To determine the postsynaptic abundance of both

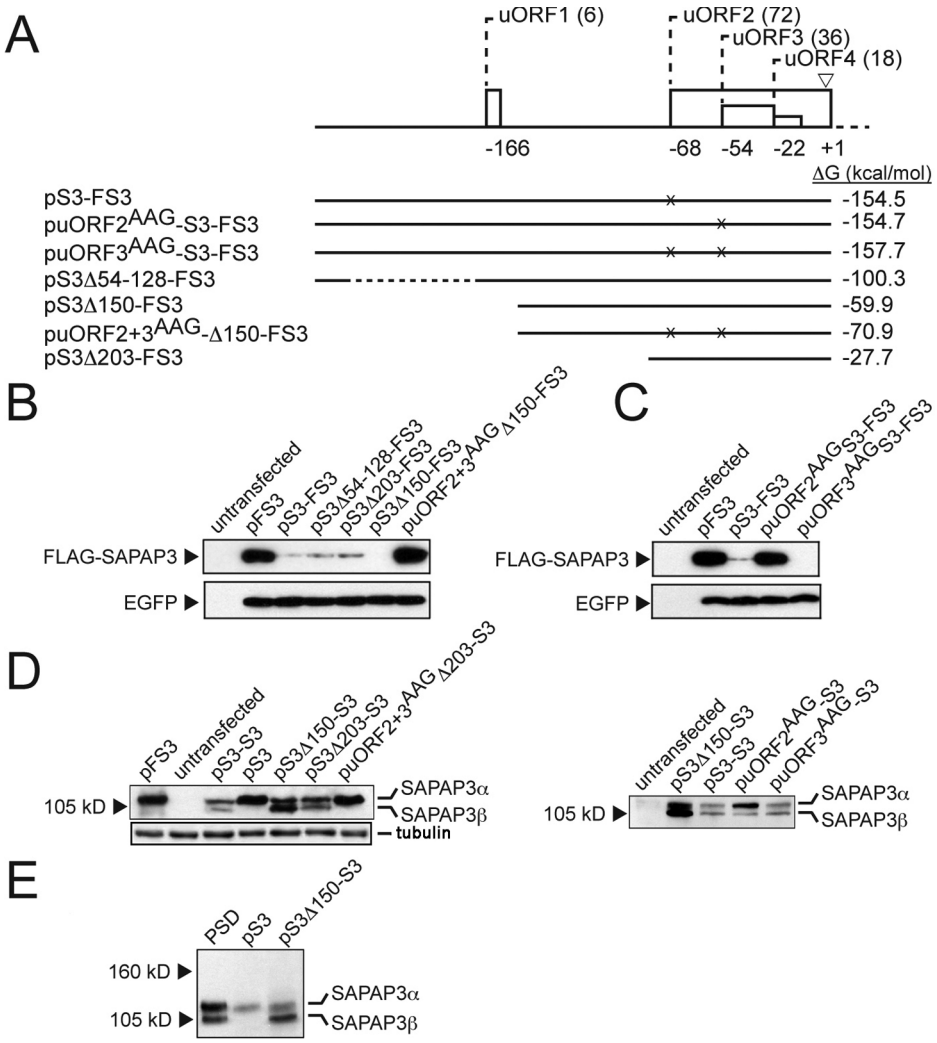

Figure 3 | uORF2 Mediates Synthesis of Two SAPAP3 Isoforms. (A) Schematic representation of the S3-5′UTR. The 5′start position (nucleotide number relative to the S3-ORF start codon (▽)) and nucleotide length (in brackets) of the four uORFs are shown. Horizontal black lines indicate regions present in transcripts encoded by the vectors listed on the left. The dotted line represents a deleted area. Positions of point mutations are indicated (×) and ΔG values of individual 5′UTRs are listed to their right. (B) Translation inhibition is independent of stable secondary structures. Protein extracts (10 μg) from untransfected and transfected HEK293 cells were analyzed by Western blotting with anti-FLAG tag and anti-EGFP antibodies. (C) Down-regulation of translation depends on an intact uORF2. Western blotting was performed as described in B. (D) Concomitant synthesis of α- and β-isoforms from authentic SAPAP3 mRNAs depends on uORF2. Western blots were performed as described in B using anti-SAPAP3 and anti-α-tubulin antibodies. (E) Two endogenous SAPAP3 isoforms co-migrating with SAPAP3α and SAPAP3β are present in a rat brain PSD fraction. Western blotting was performed as described in D.

Table 1 | Sequences surrounding putative start codons within the 5′ part of SAPAP3 mRNAs. The consensus Kozak sequence is given at the top. Putative start codons (positions +1 to +3) are underlined and consensus nucleotides at positions −3 and +4 are indicated in bold print. NetStart scores above 0.5 indicate that translation initiation is likely to occur at the respective AUG

Name	Sequences	Position	NetStart score
Kozak sequence	C$\frac{A}{G}$CCAUG**G**	n.a.	n.a.
uAUG1	CACCAUGU	−166	0.491
uAUG2	AAGGAUGG	−68	0.584
uAUG3	CCGGAUGG	−54	0.577
uAUG4	CAGUAUGA	−22	0.424
AUG^{+1}	GGGCAUGA	+1	0.754
AUG^{+67}	GCAUAUGG	+67	0.641
AUG^{+277}	CAGGAUGU	+277	0.603

SAPAP3 isoforms during brain development, we analyzed whole rat brain PSD fractions by Western blotting. Whereas SAPAP1 is already detected in embryonic brain (E20) and remains present until adulthood, its low molecular weight isoform GKAP first appears around postnatal day 21 (P21) (Fig. 5A). In contrast, both SAPAP3 isoforms progressively accumulate at PSDs during early rat brain development, a trend similarly observed for PSD-95. Noteworthy, the α:β ratio remains approximately constant throughout brain development. While postsynaptic SAPAP levels drop after P21, PSD-95 still appears to accumulate at PSD during late postnatal development. Further analysis of PSD fractions from six different adult rat brain regions revealed a strong postsynaptic accumulation of both SAPAP3 isoforms in the neocortex, hippocampus and thalamus (Fig. 5B), whereas the cerebellum, brain stem and olfactory bulb contain relatively low SAPAP3 levels. In the hippocampus, thalamus, cerebellum and brain stem, SAPAP3β is the predominant isoform with α:β ratios of 0.69, 0.59, 0.47 and 0.89, respectively. In contrast, SAPAP3α levels in the

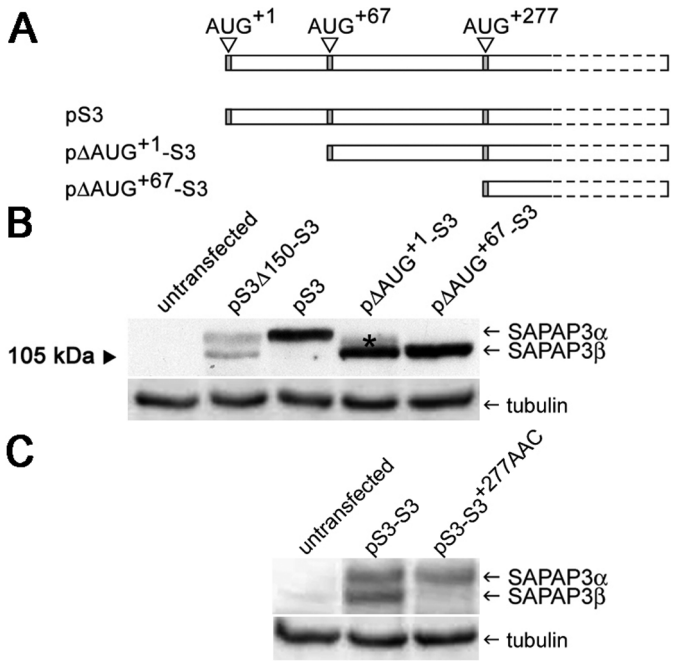

Figure 4 | SAPAP3β synthesis initiates at an internal start codon of the S3-ORF. (A) Schematic representation of the 5′ section of the S3-ORF. Boxes indicate the regions present in transcripts encoded by the vectors listed on the left. Gray boxes represent AUG triplets. (B&C) SAPAP3β synthesis starts at AUG^{+277}. Protein extracts (10 μg) from untransfected and transfected HEK293 cells were analyzed by Western blotting with an anti-SAPAP3 antiserum and anti-α-tubulin antibodies.

olfactory bulb are about 20% higher than the corresponding SAPAP3β concentration (1.19 α:β ratio) while the α:β ratio in the neocortex is about 1.

Phosphorylation at Serine 51 decreases the level of functional eIF2α by inhibiting GTP-GDP exchange and consequently limits translation initiation events[2]. In transcripts containing several uAUGs, post-termination 40 S subunits resuming 5′UTR scanning are therefore more likely to reinitiate translation at the authentic mAUG after translating a uORF. To assess whether eIF2α phosphorylation may affect relative initiation rates occurring at AUG^{+1} and AUG^{+277} of SAPAP3 mRNAs *in vivo*, we analyzed the α:β ratio in three different brain regions of heterozygous $eIF2\alpha^{+/S51A}$ knock-in mice[48]. In these animals, one eIF2α allele encodes a variant that contains an alanine instead of a serine residue at position 51 and is therefore phosphorylation resistant. Thus, heterozygous mice possess reduced phospho-eIF2α levels compared to wildtype animals. We prepared both total homogenates and PSD enriched fractions from the neocortex, hippocampus and cerebellum of individual adult wildtype and heterozygous mice. In these brain fractions, the α:β ratio was determined by Western blotting with a SAPAP3 specific antiserum. In both homogenates and PSD enriched fractions obtained from all three tested brain areas, α:β ratios were found to be unaltered in $eIF2\alpha^{+/S51A}$ knock-in animals compared to wildtype mice (Fig. 5C&D). Also we did not observe any statistically significant variations in total SAPAP3α or SAPAP3β levels (normalized against tubulin concentrations) between wildtype and knock-in mice (Fig. 5E). However, whereas α:β ratios were close to 1 in homogenates from all three brain regions and postsynaptic sites of the cerebellum, SAPAP3α is the predominant isoform in PSD fractions of the neocortex and hippocampus. Taken together, these data suggest that while in brain neurons the relative synthesis rate of SAPAP3α compared to SAPAP3β may not be influenced by the phosphorylation of eIF2α, postsynaptic α:β ratios in different brain regions may still be variable.

Discussion

In this study, we describe *cis*-acting elements regulating the translation of mRNAs encoding the postsynaptic protein SAPAP3. At excitatory mammalian brain synapses, central scaffold proteins of the PSD, such as SAPAP3, Shanks and PSD-95, cross-link glutamate receptors, signaling molecules and microfilaments[39–41,43]. Activity-induced synaptic translation of dendritic mRNAs encoding these scaffold proteins is thought to initiate a reorganization of the postsynaptic signaling machinery and thus mediate synaptic plasticity[38,41,42,44]. When entering the cytoplasm, mRNAs designated for dendritic transport are generally assumed to remain translationally dormant until specific synaptic signals trigger their local translation[27,28]. However, molecular events controlling translation initiation of particular dendritic transcripts remain poorly understood. Our data show that SAPAP3 mRNAs contain a relatively long and GC-rich 5′UTR, which does not possess IRES activity. Instead, independent of the 3′UTR, the 5′UTR strongly down-regulates translation efficiency as compared to both a short synthetic 5′-leader and the 5′UTR of SAPAP1 mRNAs, which is of equivalent length to the S3-5′UTR. Since SAPAP1 in contrast to SAPAP3 transcripts are confined to neuronal somata[33,34] the observed regulatory difference between these two mRNAs encoding similar proteins may reflect distinct translation control mechanisms employed by different neuronal subregions. In particular, it is tempting to speculate that the S3-5′UTR mediates translation silencing while the transcripts are transported to dendrites. Moreover, based upon current knowledge, the identified regulatory mechanism sets SAPAP3 mRNAs apart from other dendritic transcripts that have been shown to regulate translation via 5′-IRES elements or sequence motifs residing within the 3′UTR[49–51]. Taken together, these findings suggest that individual dendritic transcripts utilize distinct molecular mechanisms to regulate translation.

How does the S3-5′UTR mediate down-regulation of translation? Our deletion analysis shows that although long and GC-rich, the S3-5′UTR does not limit translation initiation via the formation of a stable secondary structure that stalls the linear movement of scanning 43 S complexes[9]. Furthermore, deletion or mutation of uAUG1, uAUG3 and uAUG4 does not alter translation efficiency. Consistently, all three uAUGs are surrounded by suboptimal Kozak sequences and are thus likely to be bypassed by most scanning 43 S complexes. In contrast, selective mutation of uAUG2 within the full-length S3-5′UTR strongly enhances translation initiation at the downstream mORF start codon. As uORF2 overlaps with the S3-ORF ribosomes translating uORF2 will bypass AUG^{+1} and thus be unable to synthesize full-length SAPAP3. Despite this, a significant proportion of scanning 43 S complexes can still bypass uAUG2 by leaky scanning and instead initiate translation at AUG^{+1} as evidenced by the amount of SAPAP3α synthesized from the pS3-S3 transcripts. In summary, uORF2 strongly diminishes the rate of translation initiation occurring at AUG^{+1} and thereby limits the synthesis of full-length SAPAP3. Further studies will be needed to dissect, which of the molecular control mechanisms described herein may be employed in particular subcellular regions of brain neurons.

Quite unexpectedly, full-length authentic SAPAP3 mRNAs direct the synthesis of two distinct isoforms in transfected cells. Synthesis of the lower molecular weight isoform SAPAP3β depends on the presence of the intact S3-5′UTR. Additionally, mutation of uAUG2 but not uAUG3 dramatically shifted the relative ratio of both isoforms in favor of the longer SAPAP3α. We further showed that translation initiation at AUG^{+1} and AUG^{+277} drives synthesis of SAPAP3α and SAPAP3β, respectively. Taken together these findings suggest that two distinct SAPAP3 isoforms are synthesized from a single mRNA by ATI (Fig. 6). 43 S complexes skipping uAUG2 via leaky scanning can initiate translation at AUG^{+1} hence resulting in the synthesis of SAPAP3α. In contrast, ribosomes translating uORF2 bypass AUG^{+1} and may either dissociate from the mRNA afterwards or continue to

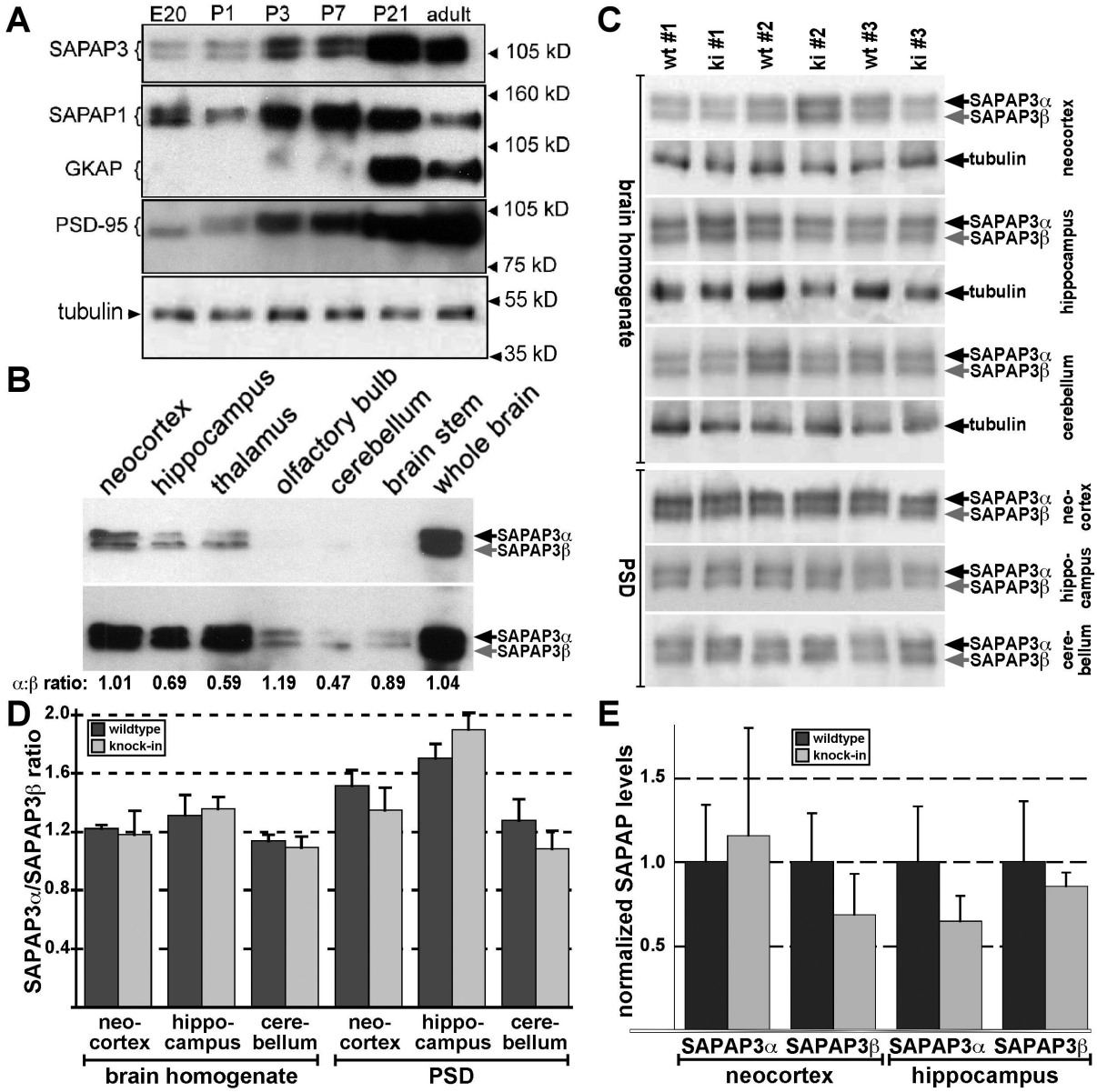

Figure 5 | Both SAPAP3 isoforms are present at PSDs. (A) Both SAPAP3α and SAPAP3β accumulate at PSDs during rat brain development. PSD fractions (2,5 μg protein) isolated from the brain of 20 days old rat embryos (E20), 1, 3, 7 and 21 days old animals (P1–P21) and adult rats were analyzed by Western blotting with an anti-SAPAP3 antiserum. (B) The α:β ratio varies in different brain regions. PSD fractions of distinct adult rat brain areas were analyzed by Western blotting as described in A. Upper and lower panels show two different exposures of the same Western blot. (C) Brain homogenates and PSD enriched fractions derived from different brain areas of each three different wildtype (wt) and heterozygous eIF2α$^{+/S51A}$ knock-in mice (ki) were used to detect both SAPAP3 isoforms and tubulin by Western blotting. (D) Bar graph indicating the ratio of SAPAP3α to SAPAP3β levels measured by Western blotting in homogenates and PSD enriched fractions obtained from the neocortex, hippocampus and cerebellum of wildtype (grey) and heterozygous eIF2α$^{+/S51A}$ knock-in mice (light grey). Variations in the SAPAP3α to SAPAP3β ratio observed in individual areas of rat (B) and wildtype mouse brains most likely reflect species specific differences. (E) Bar graph depicting total levels of SAPAP3α and SAPAP3β in different brain regions of wildtype (grey) and heterozygous eIF2α$^{+/S51A}$ knock-in animals (light grey). SAPAP3 levels were normalized against tubulin and normalized wildtype values are arbitrarily set to 1. Variations in both SAPAP3α and SAPAP3β concentrations observed between wildtype and knock-in mice are not statistically significant. See text for further details.

reinitiate translation at AUG^{+277} thereby synthesizing SAPAP3β. A similar mechanism contributes to the synthesis of two FLI-1 isoforms from a single mRNA[52]. While both AUG^{+67} and AUG^{+277} are predicted to represent equally efficient start codons, our data show that only the second triplet serves as a competent initiator site for SAPAP3β synthesis. This pronounced preference for reinitiation at AUG^{+277} as compared to AUG^{+67} may result from its larger distance from the uORF2 stop codon. As a consequence, the probability of eIF2–Met-tRNAi–GTP reloading for 40 S ribosomal subunits that resume scanning after translating uORF2 and thus become initiation competent again is much higher for AUG^{+277} relative to AUG^{+67} [7,10]. In Western blots, two endogenous rat SAPAP3 isoforms from PSD fractions co-migrated with SAPAP3α and SAPAP3β synthesized in transfected HEK293 cells. These data imply that the ATI scenario outlined above is indeed responsible for the synthesis of two distinct SAPAP3 isoforms in the rat brain. This assumption is further supported by the fact that uORF2 is highly conserved and the nucleotides surrounding AUG^{+277} including the Kozak sequence are identical in

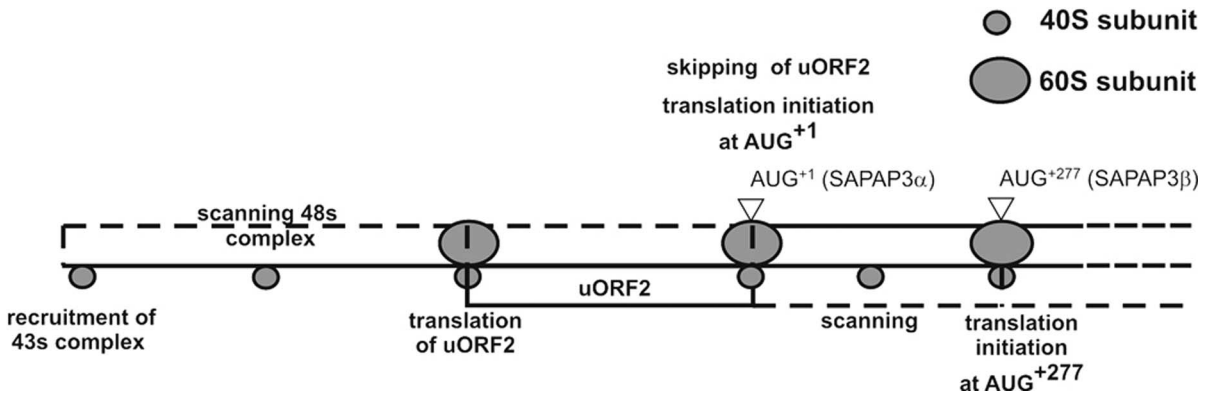

Figure 6 | Synthesis of two distinct SAPAP3 isoforms from a single mRNA. As a result of leaky scanning, some 43 S complexes will skip uAUG2 and initiate translation at AUG^{+1} thus synthesizing SAPAP3α (upper part). Alternatively, ribosomes translating uORF2 bypass AUG^{+1} and may reinitiate translation at AUG^{+277} giving rise to SAPAP3β (lower part). See text for further details.

SAPAP3 mRNAs from rat, mouse, dog and human (Figs. 1 & S3). Indeed, the mouse brain also contains two distinct SAPAP3 isoforms[34] that are no longer detected in SAPAP3 knockout mice in which a single exon containing most of uORF2, AUG^{+1} and AUG^{+277} has been deleted[44].

While phosphorylation of eIF2α reduces general translation, it enhances translation of particular mRNAs containing several uORFs[2]. Analyzing the postsynaptic α:β ratio in three different brain areas of both wildtype and $eIF2\alpha^{+/S51A}$ mice, we did not observe any genotype specific differences. These findings indicate that control over the relative synthesis of SAPAP3α to SAPAP3β from the same mRNA is not exerted by eIF2α phosphorylation. Nevertheless, it remains to be ascertained if other signaling events regulating the probability of leaky scanning or reinitiation[31] could be used to control SAPAP3α:SAPAP3β ratios in the mammalian brain and whether ratio variations in different rodent brain areas observed herein are a result of such a regulatory mechanism.

In addition to alternative splicing of pre-mRNAs, ATI represents an alternative mechanism to increase the number of isoforms, which are generated from a single gene and often possess distinct cellular functions[31]. Our data show that the 92 N-terminal amino acids of SAPAP3α, which do not encode a known domain, are missing in SAPAP3β. In SAPAP1, the N-terminal 343 amino acid residues direct selective postsynaptic targeting[53]. Our finding that both SAPAP3 isoforms are highly concentrated in PSD preparations however suggests that the unique N-terminal part of SAPAP3α is not required for trafficking to the PSD. Moreover, while the N-terminus of SAPAP1 binds neurofilaments[54] it is neither clear whether the corresponding region in SAPAP3 possesses the same capacity nor how the 92 N-terminal amino acids of SAPAP3α may influence such an interaction. Despite this lack of functional information both SAPAP3α and SAPAP3β appear to be required for normal brain function as the molecular components ensuring the synthesis of two isoforms are highly conserved in several mammalian species. As mice lacking both SAPAP3 variants display an obsessive-compulsive behavior[44] it will be interesting to test whether the selective loss of either SAPAP3α or SAPAP3β may be sufficient to cause this abnormality.

Methods

RNA preparation, polymerase chain reaction (PCR), 5′ rapid amplification of cDNA ends (5′ RACE) and Northern Blotting. RNA preparation, PCR and reverse transcription initiated PCR (RT-PCR) were performed as described[55]. PCRs to amplify 5′ UTR sequences of SAPAP3 mRNAs contained 6% (v/v) DMSO. cDNA sequences corresponding to the 5′ UTR of SAPAP3 mRNAs were amplified using oligonucleotide RA3 (CTCGGTCGCCATGGTAACCCCTC) and the SMART RACE cDNA Amplification Kit (Clontech). Total RNA from HEK293 cells was isolated using TRIzol reagent (Invitrogen) and Northern blots were generated using the glyoxal method[56]. A cDNA fragment containing nucleotides 96 to 1440 of the rat SAPAP3 cDNA (GenBank accession number NM_173138) was labeled with P^{32} using the Prime-It II Random Primer Labeling Kit (Stratagene) and used to probe Northern blots. Labeled bands were visualized using a BAS-1800II phosphoimager (Fujifilm).

Eukaryotic expression vectors. p5′S3-EGFP was constructed by inserting a cDNA region corresponding to the complete 5′UTR (Fig. 1A; GenBank accession number FJ705273) and the first 24 nucleotides of the coding region of rat SAPAP3 mRNAs (GenBank accession number AY530298) into the polylinker of pEGFP-N3 (Clontech). To generate pFS3 the EYFP coding region in pEYFP-N1 (Clontech) was replaced by a cDNA sequence encoding full-length rat SAPAP3 (GenBank accession number AY530298) tagged with an N-terminal FLAG epitope and the complete 3'UTR of rat SAPAP3 mRNAs (GenBank accession number FJ705274). cDNA sequences corresponding to the 5′UTR of rat SAPAP3 (Fig. 1A, nucleotides 1–281) and SAPAP1 mRNAs (GenBank accession number NM_022946) were inserted into pFS3 shortly upstream of the coding region to create pS3-FS3 and pS1-FS3, respectively. Vectors pS3Δ53-124-FS3, pS3Δ150-FS3 and pS3Δ203-FS3 are identical to pS3-FS3 except for deletions spanning nucleotides 53–124, 1–150 and 1–203 of the 5′UTR encoding cDNA, respectively. $puORF2^{AAG}$S3-FS3 and $puORF3^{AAG}$S3-FS3 are derivatives of pS3-FS3 containing T→A point mutations in positions 229 and 243 of the 5′UTR cDNA, respectively. $puORF2+3^{AAG}$-Δ150-FS3 is identical to pS3Δ150-FS3 but contains two T→A nucleotide exchanges in positions 229 and 243 of the 5′UTR cDNA. Replacing the EYFP cDNA in pEYFP-N1 by cDNA sequences corresponding to either the complete rat SAPAP3 mRNA or all regions except for the 5′UTR gave rise to vectors pS3-S3 and pS3, respectively. In the pS3-S3 derivatives $puORF2^{AAG}$-S3, $puORF2^{AAG}$-S3 and pS3-$S3^{+277AAC}$, the ATG triplets encoding uAUG2, uAUG3 and AUG^{+277} are mutated into AAG and AAC trinucleotides, respectively. Vectors pΔAUG^{+1}-S3 and pΔAUG^{+67}-S3 are identical to pS3 with the exception that nucleotides 1–66 and 1–276 of the coding region of the rat SAPAP3 cDNA (GenBank accession number NM_173138) are deleted, respectively. pBFS3, pBFE and pBFA are generated by exchanging the intervening sequence between *Photinus* and *Renilla* luciferase cDNAs in pBicFire[57] with cDNAs corresponding to the 5′UTR of rat SAPAP3 mRNAs or IRES elements derived from Encephalomyocarditis virus or Arc/arg3.1 transcripts, respectively[30]. Digesting pBicFire with either EcoRI and XbaI or NheI and EcoRI, treatment with Klenow polymerase (Fermentas) and ligation of vector ends with T4 DNA ligase (Fermentas) gave rise to pLUC and pREN, respectively. Vectors pS35-LUC and pS33-LUC are derivatives of pLUC in which cDNA sequences encoding either the synthetic 5′ or 3′UTR are exchanged for cDNAs corresponding to the respective regions of rat SAPAP3 mRNAs, respectively, whereas pS353-LUC contains both 5′ and 3′UTR sequences of SAPAP3 cDNAs (for 5′ and 3′UTR sequences of various mRNAs used in this study see Supplementary Table 1 online).

Animals, cell culture, transfection and luciferase assays. Wistar rats were raised in the animal facility of the University Hospital Hamburg-Eppendorf. Rat primary neurons were essentially prepared and transfected as described[58], but neurons were grown in NEUROBASAL medium (Invitrogen) without glial feeder layer and transfected seven days after plating. Growth and transfection of human embryonic kidney (HEK) 293 cells was performed as described[59]. The Dual-Luciferase Reporter Assay System (Promega) was used according to the manufacturer's recommendations with cell extracts prepared 24 hours after transfection.

Antibodies, Western blotting and PSD preparations. GST fusion proteins containing amino acid residues 694–747 and 722–776 of rat SAPAP3 and SAPAP1 were used to raise rabbit polyclonal antisera #5297 and #5280, respectively. Monoclonal antibodies directed against the FLAG epitope (Stratagene) and rabbit polyclonal antisera recognizing GFP (Abcam) are commercially available. Western

blotting was performed as described[59] with primary antibodies used at the following dilutions: affinity-purified anti-SAPAP3 (#5297), 1 : 2000; affinity-purified anti-SAPAP1 (#5280), 1 : 66; anti-FLAG, 1 : 2000; anti-GFP, 1 : 10000. PSD[60] and PSD enriched fractions[61] were essentially prepared as described, snap frozen in liquid nitrogen and stored at −80°C.

Animals welfare. Experimental animals were bred at the animal facility of the McGill Life Sciences Complex, Montréal, Canada and handled in accordance with national guidelines for animal welfare. All studies were approved by the Mc Gill University animal committee.

Nucleotide sequence GenBank accession numbers. 5′ and 3′ UTR sequences of rat cDNA sequences encoding 5′ and 3′ UTRs of the rat SAPAP3 mRNA, respectively, were deposited in the GenBank database under the accession numbers FJ705273 and FJ705274, respectively.

1. Topisirovic, I., Svitkin, Y. V., Sonenberg, N. & Shatkin, A. J. Cap and cap-binding proteins in the control of gene expression. *Wiley Interdiscip Rev RNA* **2**, 277–298 (2011).
2. Sonenberg, N. & Hinnebusch, A. G. Regulation of translation initiation in eukaryotes: mechanisms and biological targets. *Cell* **136**, 731–745 (2009).
3. Kozak, M. An analysis of 5′-noncoding sequences from 699 vertebrate messenger RNAs. *Nucleic Acids Res* **15**, 8125–8148 (1987).
4. Kozak, M. At least six nucleotides preceding the AUG initiator codon enhance translation in mammalian cells. *J Mol Biol* **196**, 947–950 (1987).
5. Kozak, M. Pushing the limits of the scanning mechanism for initiation of translation. *Gene* **299**, 1–34 (2002).
6. Kozak, M. Recognition of AUG and alternative initiator codons is augmented by G in position +4 but is not generally affected by the nucleotides in positions +5 and +6. *EMBO J.* **16**, 2482–2492 (1997).
7. Wethmar, K., Smink, J. J. & Leutz, A. Upstream open reading frames: molecular switches in (patho)physiology. *Bioessays* **32**, 885–893 (2010).
8. Myers, S. J., Huang, Y., Genetta, T. & Dingledine, R. Inhibition of glutamate receptor 2 translation by a polymorphic repeat sequence in the 5′-untranslated leaders. *J Neurosci* **24**, 3489–3499 (2004).
9. Kozak, M. Structural features in eukaryotic mRNAs that modulate the initiation of translation. *J Biol Chem* **266**, 19867–19870 (1991).
10. Meijer, H. A. & Thomas, A. A. Control of eukaryotic protein synthesis by upstream open reading frames in the 5′-untranslated region of an mRNA. *Biochem J* **367**, 1–11 (2002).
11. Hughes, T. A. & Brady, H. J. Expression of axin2 is regulated by the alternative 5′-untranslated regions of its mRNA. *J Biol Chem* **280**, 8581–8588 (2005).
12. Ghilardi, N., Wiestner, A. & Skoda, R. C. Thrombopoietin production is inhibited by a translational mechanism. *Blood* **92**, 4023–4030 (1998).
13. Vattem, K. M. & Wek, R. C. Reinitiation involving upstream ORFs regulates ATF4 mRNA translation in mammalian cells. *Proc Natl Acad Sci U S A* **101**, 11269–11274 (2004).
14. Lu, P. D., Harding, H. P. & Ron, D. Translation reinitiation at alternative open reading frames regulates gene expression in an integrated stress response. *J Cell Biol* **167**, 27–33 (2004).
15. Grant, C. M., Miller, P. F. & Hinnebusch, A. G. Requirements for intercistronic distance and level of eukaryotic initiation factor 2 activity in reinitiation on GCN4 mRNA vary with the downstream cistron. *Mol Cell Biol* **14**, 2616–2628 (1994).
16. Kozak, M. Effects of intercistronic length on the efficiency of reinitiation by eucaryotic ribosomes. *Mol Cell Biol* **7**, 3438–3445 (1987).
17. Kozak, M. Constraints on reinitiation of translation in mammals. *Nucleic Acids Res* **29**, 5226–5232 (2001).
18. Poyry, T. A., Kaminski, A. & Jackson, R. J. What determines whether mammalian ribosomes resume scanning after translation of a short upstream open reading frame? *Genes Dev.* **18**, 62–75 (2004).
19. Calkhoven, C. F., Muller, C. & Leutz, A. Translational control of C/EBPalpha and C/EBPbeta isoform expression. *Genes Dev.* **14**, 1920–1932 (2000).
20. Leissring, M. A. *et al.* Alternative translation initiation generates a novel isoform of insulin-degrading enzyme targeted to mitochondria. *Biochem J* **383**, 439–446 (2004).
21. Hinnebusch, A. G. Translational regulation of GCN4 and the general amino acid control of yeast. *Annu. Rev. Microbiol.* **59**, 407–450 (2005).
22. Takei, N., Kawamura, M., Hara, K., Yonezawa, K. & Nawa, H. Brain-derived neurotrophic factor enhances neuronal translation by activating multiple initiation processes: comparison with the effects of insulin. *J Biol Chem* **276**, 42818–42825 (2001).
23. Costa-Mattioli, M. *et al.* Translational control of hippocampal synaptic plasticity and memory by the eIF2alpha kinase GCN2. *Nature* **436**, 1166–1173 (2005).
24. Costa-Mattioli, M. *et al.* eIF2alpha phosphorylation bidirectionally regulates the switch from short- to long-term synaptic plasticity and memory. *Cell* **129**, 195–206 (2007).
25. Doyle, M. & Kiebler, M. A. Mechanisms of dendritic mRNA transport and its role in synaptic tagging. *EMBO J.* **30**, 3540–3552 (2011).
26. Bramham, C. R. & Wells, D. G. Dendritic mRNA: transport, translation and function. *Nat Rev Neurosci* **8**, 776–789 (2007).
27. Cajigas, I. J., Will, T. & Schuman, E. M. Protein homeostasis and synaptic plasticity. *EMBO J.* **29**, 2746–2752 (2010).
28. Swanger, S. A. & Bassell, G. J. Making and breaking synapses through local mRNA regulation. *Curr. Opin. Genet. Dev.* **21**, 414–421 (2011).
29. Kindler, S. & Kreienkamp, H. J. The role of the postsynaptic density in the pathology of the fragile x syndrome. *Results Probl. Cell Differ.* **54**, 61–80 (2011).
30. Pinkstaff, J. K., Chappell, S. A., Mauro, V. P., Edelman, G. M. & Krushel, L. A. Internal initiation of translation of five dendritically localized neuronal mRNAs. *Proc Natl Acad Sci U S A* **98**, 2770–2775 (2001).
31. Jackson, R. J. Alternative mechanisms of initiating translation of mammalian mRNAs. *Biochem Soc Trans* **33**, 1231–1241 (2005).
32. Pisarev, A. V., Shirokikh, N. E. & Hellen, C. U. Translation initiation by factor-independent binding of eukaryotic ribosomes to internal ribosomal entry sites. *C R Biol* **328**, 589–605 (2005).
33. Kindler, S., Rehbein, M., Classen, B., Richter, D. & Böckers, T. M. Distinct spatiotemporal expression of SAPAP transcripts in the developing rat brain: a novel dendritically localized mRNA. *Brain Res Mol Brain Res* **126**, 14–21 (2004).
34. Welch, J. M., Wang, D. & Feng, G. Differential mRNA expression and protein localization of the SAP90/PSD-95-associated proteins (SAPAPs) in the nervous system of the mouse. *J Comp Neurol* **472**, 24–39 (2004).
35. Böckers, T. M. *et al.* Differential expression and dendritic transcript localization of Shank family members: identification of a dendritic targeting element in the 3′ untranslated region of Shank1 mRNA. *Mol Cell Neurosci* **26**, 182–190 (2004).
36. Zalfa, F. *et al.* A new function for the fragile X mental retardation protein in regulation of PSD-95 mRNA stability. *Nat Neurosci* **10**, 578–587 (2007).
37. Muddashetty, R. S., Kelic, S., Gross, C., Xu, M. & Bassell, G. J. Dysregulated metabotropic glutamate receptor-dependent translation of AMPA receptor and postsynaptic density-95 mRNAs at synapses in a mouse model of fragile X syndrome. *J Neurosci* **27**, 5338–5348 (2007).
38. Gundelfinger, E. D., Boeckers, T. M., Baron, M. K. & Bowie, J. U. A role for zinc in postsynaptic density asSAMbly and plasticity? *Trends Biochem Sci* **31**, 366–373 (2006).
39. Okabe, S. Molecular anatomy of the postsynaptic density. *Mol Cell Neurosci* **34**, 503–518 (2007).
40. Sheng, M. & Hoogenraad, C. C. The postsynaptic architecture of excitatory synapses: a more quantitative view. *Annu Rev Biochem* **76**, 823–847 (2007).
41. Chua, J. J., Kindler, S., Boyken, J. & Jahn, R. The architecture of an excitatory synapse. *J. Cell Sci.* **123**, 819–823 (2010).
42. Kreienkamp, H. J. Scaffolding proteins at the postsynaptic density: shank as the architectural framework. *Handb Exp Pharmacol* 365–380 (2008).
43. van Spronsen, M. & Hoogenraad, C. C. Synapse pathology in psychiatric and neurologic disease. *Curr Neurol Neurosci Rep* **10**, 207–214 (2010).
44. Welch, J. M. *et al.* Cortico-striatal synaptic defects and OCD-like behaviours in Sapap3-mutant mice. *Nature* **448**, 894–900 (2007).
45. Mazumder, B., Seshadri, V., Imataka, H., Sonenberg, N. & Fox, P. L. Translational silencing of ceruloplasmin requires the essential elements of mRNA circularization: poly(A) tail, poly(A)-binding protein, and eukaryotic translation initiation factor 4G. *Mol Cell Biol* **21**, 6440–6449 (2001).
46. Kuersten, S. & Goodwin, E. B. The power of the 3′ UTR: translational control and development. *Nat Rev Genet* **4**, 626–637 (2003).
47. Wilkie, G. S., Dickson, K. S. & Gray, N. K. Regulation of mRNA translation by 5′- and 3′-UTR-binding factors. *Trends Biochem Sci* **28**, 182–188 (2003).
48. Scheuner, D. *et al.* Translational control is required for the unfolded protein response and in vivo glucose homeostasis. *Mol. Cell* **7**, 1165–1176 (2001).
49. Wu, L. *et al.* CPEB-mediated cytoplasmic polyadenylation and the regulation of experience-dependent translation of alpha-CaMKII mRNA at synapses. *Neuron* **21**, 1129–1139 (1998).
50. Shin, C. Y., Kundel, M. & Wells, D. G. Rapid, activity-induced increase in tissue plasminogen activator is mediated by metabotropic glutamate receptor-dependent mRNA translation. *J Neurosci* **24**, 9425–9433 (2004).
51. Hüttelmaier, S. *et al.* Spatial regulation of beta-actin translation by Src-dependent phosphorylation of ZBP1. *Nature* **438**, 512–515 (2005).
52. Sarrazin, S. *et al.* Negative and translation termination-dependent positive control of FLI-1 protein synthesis by conserved overlapping 5′ upstream open reading frames in Fli-1 mRNA. *Mol Cell Biol* **20**, 2959–2969 (2000).
53. Yao, I., Iida, J., Nishimura, W. & Hata, Y. Synaptic localization of SAPAP1, a synaptic membrane-associated protein. *Genes Cells* **8**, 121–129 (2003).
54. Hirao, K. *et al.* Association of synapse-associated protein 90/postsynaptic density-95-associated protein (SAPAP) with neurofilaments. *Genes Cells* **5**, 203–210 (2000).
55. Monshausen, M. *et al.* Two rat brain staufen isoforms differentially bind RNA. *J Neurochem* **76**, 155–165 (2001).
56. Sambrook, J., Fritsch, E. F. & Maniatis, T. *Molecular Cloning: A Laboratory Manual* (Cold Spring Harbor Laboratory Press, Cold Spring Harbor, NY, 1989).
57. Pedersen, S. K., Christiansen, J., Hansen, T. O., Larsen, M. R. & Nielsen, F. C. Human insulin-like growth factor II leader 2 mediates internal initiation of translation. *Biochem J* **363**, 37–44 (2002).
58. Blichenberg, A. *et al.* Identification of a cis-acting dendritic targeting element in MAP2 mRNAs. *J Neurosci* **19**, 8818–8829 (1999).

59. Monshausen, M., Rehbein, M., Richter, D. & Kindler, S. The RNA-binding protein Staufen from rat brain interacts with protein phosphatase-1. *J Neurochem* **81**, 557–564 (2002).
60. Carlin, R. K., Grab, D. J., Cohen, R. S. & Siekevitz, P. Isolation and characterization of postsynaptic densities from various brain regions: enrichment of different types of postsynaptic densities. *J Cell Biol* **86**, 831–845 (1980).
61. Coba, M. P. *et al*. Neurotransmitters drive combinatorial multistate postsynaptic density networks. *Sci Signal* **2**, ra19 (2009).

Acknowledgements

Financial support from the Deutsche Forschungsgemeinschaft (Ki488/2-6 to M.R. and S.K. and KR1321/4-1 to S.K.) and Thyssen-Stiftung (Az. 10.05.2.185 to D.R. and S.K.) is acknowledged.

Author contributions

JJEC and SK conceived and designed the project with input from MR and DR. JJEC, CS, CGG and SK performed experiments. JJEC and SK wrote the manuscript, with contributions from all authors.

Additional information

Supplementary information accompanies this paper at http://www.nature.com/scientificreports

Competing financial interests: The authors declare no competing financial interests.

License: This work is licensed under a Creative Commons Attribution-NonCommercial-ShareAlike 3.0 Unported License. To view a copy of this license, visit http://creativecommons.org/licenses/by-nc-sa/3.0/

How to cite this article: Chua, J.J.E. *et al*. Synthesis of two SAPAP3 isoforms from a single mRNA is mediated via alternative translational initiation. *Sci. Rep.* **2**, 484; DOI:10.1038/srep00484 (2012).